Theoretical and experimental investigations of coherent phonon dynamics in sapphire crystal using femtosecond time-resolved coherent anti-Stokes Raman scattering*

Du Xin(杜 鑫)[a)b)], Zhang Ming-Fu(张明福)[c)], He Xing(何 兴)[a)], Meng Qing-Kun(孟庆琨)[a)], Song Yun-Fei(宋云飞)[a)], Yang Yan-Qiang(杨延强)[a)†], and Han Jie-Cai(韩杰才)[c)]

[a)] *Centre for Condensed Matter Science and Technology, Department of Physics, Harbin Institute of Technology, Harbin* 150080, *China*

[b)] *College of Foundation Science, Harbin University of Commerce, Harbin* 150028, *China*

[c)] *Centre for Composite Materials, Harbin Institute of Technology, Harbin* 150080, *China*

(Received 26 February 2011; revised manuscript received 14 June 2011)

We report on the theoretical and the experimental investigations of the coherent phonon dynamics in sapphire crystal using the femtosecond time-resolved coherent anti-Stokes Raman scattering (fs-CARS) technique. The temporal chirped white-light continuum (WLC) is used for the Stokes pulse, therefore we can perform the selective excitation of the phonon modes without using a complicated laser system. The expected quantum beat phenomenon is clearly observed. The theoretical formulas consist very well with the experimental results. The dephasing times of the excited phonon modes, the wavenumber difference, and the phase shift between the simultaneously excited modes are obtained and discussed. This work opens up a way to study directly high-frequency coherent phonon dynamics in bulk crystals on a femtosecond time scale and is especially helpful for understanding the nature of coherent phonons.

Keywords: coherent phonon, femtosecond time-resolved coherent anti-Stokes Raman scattering, dephasing, quantum beat

PACS: 63.20.–e, 42.65.Dr, 42.50.Md, 78.47.jh **DOI:** 10.1088/1674-1056/20/12/126301

1. Introduction

With the advances in femtosecond laser technology, one can directly excite and detect coherent phonons with very fast dephasing times in the time domain. By employing femtosecond pump-probe reflection or transmission measurements, the studies of the dynamics of coherent phonons have been performed in various materials, such as semimetals,[1−3] semiconductors,[4−7] superconductors,[8] and semiconductor quantum dots.[9] However, the valuable femtosecond pump-probe technique requires that laser pulse duration should be sufficiently smaller than the period of the coherent lattice vibrations, and it is suited for studying low-frequency phonon modes. The application is actually limited by several factors, for example, phonon dynamics appears as decaying oscillatory components, the phonon information is obtained by the Fourier transform. Therefore, the sensitivity and frequency-resolution in the pump-probe technique are low especially for high-frequency phonons because of the limitation of laser pulse duration. On the contrary, femtosecond time-resolved coherent anti-Stokes Raman scattering (fs-CARS) technique has proved to be a powerful tool for studying high-frequency vibrational modes. Furthermore, there are both practical and fundamental considerations in time-frequency two-dimensional spectroscopy for more detailed dynamical studies. This technique has been widely used in liquid phase and gas phase materials.[10−18] However, with the development of applied technique and basic research, the knowledge of the dynamics of high-frequency coherent phonons in crystals is required. For example, it has been reported that the measurements of dephasing times of coherent phonons can be used to investigate the behaviours of the defects in bulk crystal.[19] Therefore, the systematic theoretical and experimental investi-

*Project supported by the National Natural Science Foundation of China (Grant No. 20973050).

†Corresponding author. E-mail: yqyang@hit.edu.cn

© 2011 Chinese Physical Society and IOP Publishing Ltd

gations of high-frequency coherent phonon dynamics in bulk crystals by using fs-CARS technique are necessary in order to compensate the deficiency in this research field.

In this paper, we present the theoretical description of using fs-CARS technique to study coherent phonon dynamics in crystals, and we also give the experimental details and experimental results of a sapphire sample as examples. In the experimental part, the temporal chirped white-light continuum (WLC) is used for the Stokes pulse, therefore the selective excitation of the phonon modes can be performed without using a complicated laser system (e.g. two dye lasers or two optical parametric amplifiers (OPA) are usually required in a similar experimental setup). The phonon modes are selectively excited, and the quantum coherence is obtained in the fs-CARS signal. The theoretical formulas are consistent with the experimental results. The dephasing times of the excited phonon modes, the wavenumber difference and phase shift between the simultaneously excited modes are determined and discussed. This work is especially helpful for understanding the nature of coherent phonons, and provides an easier way to implement the study of high-frequency coherent phonon dynamics in bulk crystals on a femtosecond time scale.

2. Theoretical description

In the measurement of fs-CARS, the sample is first subjected to two synchronized laser pulses with frequencies $\omega_{\rm p}$ and $\omega_{\rm s}$ and wave vectors $\boldsymbol{k}_{\rm p}$ and $\boldsymbol{k}_{\rm s}$ used as pump and Stokes pulses, respectively. If the frequency difference $\omega_{\rm p}-\omega_{\rm s}$ is equal to the frequency ω_0 of a specific phonon mode, this mode will be resonantly excited. The temporal evolution of the coherent lattice vibrations is monitored by the third time-delayed probe pulse with frequency $\omega_{\rm pr}$ (usually $\omega_{\rm pr}=\omega_{\rm p}$) and wave vector $\boldsymbol{k}_{\rm pr}$, giving rise to a CARS signal with frequency $\omega_{\rm c}=\omega_{\rm p}-\omega_{\rm s}+\omega_{\rm pr}$ and wave vector $\boldsymbol{k}_{\rm c}=\boldsymbol{k}_{\rm p}-\boldsymbol{k}_{\rm s}+\boldsymbol{k}_{\rm pr}$. The CARS signal was recorded as a function of the delay time τ between the probe pulse and the synchronous pump and Stokes pulses. The dephasing time T_2 of the coherent phonons can be deduced from the temporal evolution of the CARS signal. It is clear that the fs-CARS technique is perfectly suited for the selective excitation of phonon modes by adjusting the frequency difference between the pump and Stokes pulses.

The propagation of the CARS light field $\boldsymbol{E}_{\rm c}(r,t)$ and its interaction with the surrounding medium is represented by the nonlinear wave equation[20,21]

$$\begin{aligned}&\boldsymbol{\nabla}\times\boldsymbol{\nabla}\times\boldsymbol{E}_{\rm c}(r,t)+\frac{n^2}{c^2}\frac{\partial^2}{\partial t^2}\boldsymbol{E}_{\rm c}(r,t)\\&=-\frac{4\pi}{c^2}\frac{\partial^2}{\partial t^2}\boldsymbol{P}_{\rm c}^{\rm NL}(r,t),\end{aligned}\tag{1}$$

where c is the speed of light and n is the refractive index. The CARS signal is generated from the nonlinear polarization $\boldsymbol{P}_{\rm c}^{\rm NL}$, which describes the light-matter interaction. For a Raman resonance process, we divide $\boldsymbol{P}_{\rm c}^{\rm NL}$ into two parts: a fast nonresonant part $\boldsymbol{P}_{\rm NR}^{\rm NL}$ due to the response of the electronic system and a slow resonant part $\boldsymbol{P}_{\rm R}^{\rm NL}$ due to the contribution of the excited coherent phonons. Thus,

$$\begin{aligned}\boldsymbol{P}_{\rm c}^{\rm NL}&=\boldsymbol{P}_{\rm R}^{\rm NL}+\boldsymbol{P}_{\rm NR}^{\rm NL}\\&=NR_{\rm a}Q\boldsymbol{E}_{\rm pr}+3\tilde{\chi}_{\rm NR}^{(3)}\boldsymbol{E}_{\rm p}\boldsymbol{E}_{\rm s}^{*}\boldsymbol{E}_{\rm pr},\end{aligned}\tag{2}$$

where Q denotes the coherent amplitude of the phonon mode, $R_{\rm a}$ is the Raman susceptibility, N is the number of primitive cells per unit volume, and $\tilde{\chi}_{\rm NR}^{(3)}$ is the nonresonant third-order nonlinear electronic susceptibility.

For the phonon mode with frequency ω_0, the coherent amplitude Q obeys the equation of motion

$$\frac{\partial^2}{\partial t^2}Q+\frac{2}{T_2}\frac{\partial}{\partial t}Q+\omega_0^2Q=\frac{1}{m}R_{\rm a}\boldsymbol{E}_{\rm p}\boldsymbol{E}_{\rm s}^{*},\tag{3}$$

where m is the reduced lattice mass and T_2 is the dephasing time of coherent phonons.

The electric fields of the pump, Stokes, probe, and CARS pulses can be written as

$$\begin{aligned}\boldsymbol{E}_{\rm p}(\boldsymbol{r},t)&=\boldsymbol{E}_{\rm p}(t)\exp(\mathrm{i}\boldsymbol{k}_{\rm p}\cdot\boldsymbol{r}),\\\boldsymbol{E}_{\rm s}(\boldsymbol{r},t)&=\boldsymbol{E}_{\rm s}(t)\exp(\mathrm{i}\boldsymbol{k}_{\rm s}\cdot\boldsymbol{r}),\\\boldsymbol{E}_{\rm pr}(\boldsymbol{r},t)&=\boldsymbol{E}_{\rm pr}(t)\exp(\mathrm{i}\boldsymbol{k}_{\rm pr}\cdot\boldsymbol{r}),\\\boldsymbol{E}_{\rm c}(\boldsymbol{r},t)&=\boldsymbol{E}_{\rm c}(t)\exp(\mathrm{i}\boldsymbol{k}_{\rm c}\cdot\boldsymbol{r}),\end{aligned}\tag{4}$$

where

$$\begin{aligned}\boldsymbol{E}_{\rm p}(t)&=\frac{1}{2}e\boldsymbol{E}_{\rm p}^{0}f_{\rm p}(t)\exp(-\mathrm{i}\omega_{\rm p}t),\\\boldsymbol{E}_{\rm s}(t)&=\frac{1}{2}e\boldsymbol{E}_{\rm s}^{0}f_{\rm s}(t)\exp(-\mathrm{i}\omega_{\rm s}t),\\\boldsymbol{E}_{\rm pr}(t)&=\frac{1}{2}e\boldsymbol{E}_{\rm pr}^{0}f_{\rm pr}(t-\tau)\exp[-\mathrm{i}\omega_{\rm p}(t-\tau)].\end{aligned}\tag{5}$$

Here e is the unit polarization vector, which is the same for all the fields in our experiment, $\boldsymbol{E}_{\rm p}^{0}$, $\boldsymbol{E}_{\rm s}^{0}$, and $\boldsymbol{E}_{\rm pr}^{0}$ denote the amplitudes of the laser pulses, and $f(t)$ is the time-dependent pulse envelope function centred at $t=0$ (for $\boldsymbol{E}_{\rm p}$ and $\boldsymbol{E}_{\rm s}$) and at the delay time τ (for $\boldsymbol{E}_{\rm pr}$). For all the incident laser pulses, the envelope functions are assumed to be Gaussian with equal

pulse duration Δt, i.e. $f(t) = \exp\left(-2\ln 2\,(t/\Delta t)^2\right)$, where Δt is the full width at half maximum (FWHM) of the laser pulse.

In a manner similar to that used for light fields, we write for the coherent amplitude

$$Q(\boldsymbol{r},t) = Q(t)\exp(\mathrm{i}\boldsymbol{k}_0\cdot\boldsymbol{r}). \tag{6}$$

For the coherent amplitude Q, equation (3) predicts the exponential decay with the time constant T_2. The $Q(t)$ can be written with the following time dependence

$$Q(t) \propto Q_0\exp(-t/T_2 - \mathrm{i}\omega_0 t + \mathrm{i}\varphi), \tag{7}$$

where φ is the phase factor of the excited phonon mode.

Substituting Eqs. (4) and (6) into Eqs. (1) and (2), and neglecting second order derivatives of the slowly varying amplitudes yield the expression

$$\begin{aligned}&\left(\frac{\partial}{\partial\boldsymbol{r}} + \frac{1}{v_\mathrm{c}}\frac{\partial}{\partial t}\right)\boldsymbol{E}_\mathrm{c}\\ &= \frac{2\pi\omega_\mathrm{c}^2}{c^2\boldsymbol{k}_\mathrm{c}}\left(NR_\mathrm{a}Q\boldsymbol{E}_\mathrm{pr} + 3\tilde{\chi}^{(3)}_\mathrm{NR}\boldsymbol{E}_\mathrm{p}\boldsymbol{E}_\mathrm{s}^*\boldsymbol{E}_\mathrm{pr}\right)\\ &\quad\times\exp(\mathrm{i}\Delta\boldsymbol{k}\cdot\boldsymbol{r}),\end{aligned} \tag{8}$$

where $\Delta\boldsymbol{k} = \boldsymbol{k}_\mathrm{c} - (\boldsymbol{k}_\mathrm{p} - \boldsymbol{k}_\mathrm{s} + \boldsymbol{k}_\mathrm{pr})$ is the k-mismatch of the probe process.

The time-integrated CARS signal intensity is measured as a function of the delay time τ between the probe and exciting pulses. Integrating Eq. (8), we obtain

$$\begin{aligned}&I_\mathrm{c}(\tau) \propto \int_{-\infty}^{+\infty}|\boldsymbol{E}_\mathrm{c}(\tau,t)|^2\,\mathrm{d}t\\ &= S\left(\frac{2\pi\omega_\mathrm{c}^2 L}{c^2\boldsymbol{k}_\mathrm{c}}\right)^2\int_{-\infty}^{+\infty}\mathrm{d}t\Big|\boldsymbol{E}_\mathrm{pr}(t-\tau)\,[NR_\mathrm{a}Q(t)\\ &\quad + 3\tilde{\chi}^{(3)}_\mathrm{NR}\boldsymbol{E}_\mathrm{p}(t)\,\boldsymbol{E}_\mathrm{s}^*(t)\Big]\Big|^2,\end{aligned} \tag{9}$$

where $S = \sin^2(\Delta kL/2)/(\Delta kL/2)^2$; L denotes the effective length of the spatial overlap of the pump, Stokes, and probe laser pulses within the sample. The factor S goes to unity as the phase mismatch $\Delta\boldsymbol{k}$ goes to zero. The $Q(t)$ is calculated from Eqs. (3) and (6).

According to Eqs. (7) and (9), if there is only one phonon mode excited by the time-coincident pump and Stokes pulses, the fs-CARS signal will show a single unmodulated exponential decay. When the neighbouring Raman levels are close enough, because of the large spectral bandwidth of the femtosecond laser pulses, two or more phonon modes will be excited simultaneously, the signal decay becomes more complex.[22] Quantum beat phenomenon originating from the interference of different phonon modes can be observed. The different modes j have the individual parameters: resonance frequencies ω_{0j}, phase factors φ_j, coherent amplitudes Q_j, and dephasing times T_{2j}. In Eq. (9), the CARS field is the sum of the light fields originating from all the excited phonon modes, i.e.,

$$\boldsymbol{E}_\mathrm{c}(\tau,t) = \sum_j \boldsymbol{E}_{\mathrm{c}j}(\tau,t). \tag{10}$$

We replace Q by the total coherent amplitude Q_tot, which is represented by the coherent superposition of individual excited phonon modes of number density N_j, i.e.,

$$Q_\mathrm{tot} = \sum_j N_j Q_j/N, \tag{11}$$

where $N = \sum_j N_j$ represents the total number density of all the excited modes.

According to Eqs. (2) and (9), the transient fs-CARS signal has two components, nonresonant and resonant. The nonresonant part of the signal gives an instantaneous electronic response of the sample, i.e. it follows the product $\boldsymbol{E}_\mathrm{p}\boldsymbol{E}_\mathrm{s}^*\boldsymbol{E}_\mathrm{pr}$ and decays very rapidly with the time resolution of the experiment. This part does not provide any information about the coherent phonons. In contrast, the resonant part, which shows slow decay, describes the signal scattered from the excited coherent phonon modes and provides information about the dynamic properties of the coherent phonon modes. The nonresonant and the resonant components of the fs-CARS signal can be clearly seen from the time evolution of $I_\mathrm{c}(\tau)$. The relative contributions of the two components are determined by $\boldsymbol{E}_\mathrm{p}(t)\boldsymbol{E}_\mathrm{s}^*(t)$ and $Q_\mathrm{tot}(t)$ according to the respective weighting factors $\tilde{\chi}^{(3)}_\mathrm{NR}$ and NR_a.

3. Experiment

A large-sized sapphire crystal was grown by SAPMAC (sapphire growth technique with micro-pulling and shoulder-expanding at cooled centre) method.[23] The sapphire crystal plate with a size of ϕ36 mm×2 mm used in the fs-CARS experiment was prepared by cutting the as-grown large sapphire crystal in the direction perpendicular to the c axis, and both its sides were polished.

Based on the space group D_{3d}^6 symmetry of corundum, group theory predicts that there are seven Raman active phonon modes $2\mathrm{A}_{1\mathrm{g}}+5\mathrm{E}_\mathrm{g}$ for sapphire. Figure 1 shows the measured Raman spectrum for

our sapphire crystal at room temperature. There are seven phonon modes with peaks located at 379, 418, 431, 450, 577, 645, and 750 cm^{-1}, which are consistent with the results reported in the literature.[24,25] According to the assignment of phonon modes, 418 cm^{-1} and 645 cm^{-1} correspond to A_{1g} phonons; 379, 431, 450, 577, and 750 cm^{-1} correspond to E_g phonons. The 379, 418, 431, and 450 cm^{-1} modes are related to the bending vibrations of $[AlO_6]$ group, and 418 cm^{-1} mode is due to the O–Al–O symmetric bending vibration. In contrast, the 577, 645, and 750 cm^{-1} modes are related to the stretching vibrations of $[AlO_6]$ group, and 645 cm^{-1} mode is attributed to the Al–O symmetric stretching vibration.

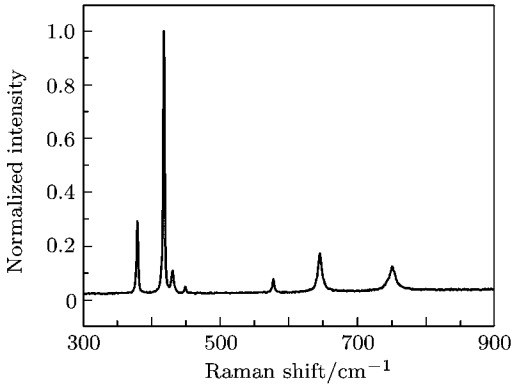


Fig. 1. Raman spectrum of our sapphire crystal.

We perform our fs-CARS measurement at room temperature. A schematic diagram of the experimental setup is illustrated in Fig. 2(a). The output pulse of about 110-fs duration centred at 800 nm from the regenerative amplifier (Spectra-Physics, Spitfire) with a repetition rate of 1 kHz and a single pulse energy of 500 μJ is split into three parts by two beam splitters (BS). Two of them are used as the pump and probe pulses of equal wavelength, and the third one is focused into a 4-mm thick Al_2O_3 crystal to produce a WLC used for the Stokes pulse. Two delay lines are employed. Figure 2(b) shows the time sequence of the three laser pulses. The WLC pulse defines an arbitrary temporal zero point. One delay line is used to produce the temporal overlap of the pump and Stokes pulse by varying the delay time between the pump and WLC pulses. The second one provides the variable time delay for the probe pulse. The pump, Stokes, and probe pulses are focused onto the sample (focal spot diameter ∼300 μm) using a lens of 300-mm focal length. The WLC has an ultrabroadband spectral profile, ranging from 300 nm to 1100 nm. Based on the temporal chirp characteristics of the WLC, the frequency difference between the pump and Stokes pulses can be tuned by changing the delay time between the pump and WLC pulses. Therefore, the selective excitation of a wide range of phonon modes can be accomplished.[10]

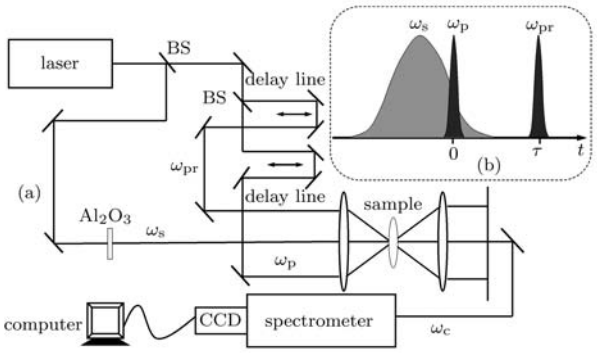


Fig. 2. Experimental setup of the fs-CARS (a), and time sequence of three laser pulses (b).

The large bandwidth of the femtosecond laser pulses and the close vibrational levels provide the opportunity to observe the quantum beat phenomenon on a terahertz scale. Firstly, we focus our attention on the high-frequency 645-cm^{-1} A_{1g} phonon and 750-cm^{-1} E_g phonon. The temporal overlap between the pump and Stokes pulses is exactly tuned to accomplish the simultaneous excitation of two objective phonon modes. In order to suppress the excitation of other modes and the generation of the degenerate four-wave mixing process, the WLC is spectrally filtered to cut off the components of wavelength less than 830 nm.

In the Raman spectrum, the 379-cm^{-1} E_g phonon and 418-cm^{-1} A_{1g} phonon display the strongest peaks. However, if the frequency difference between the pump pulse and the Stokes pulse is adjusted to match these two modes, a spectral overlap of the pulses is generated because of the broad bandwidth of femtosecond laser pulses. This results in a huge degenerate four-wave mixing (DFWM) signal at the spectral position of the pump pulse, since this process is several orders of magnitude more efficient than the CARS process. Due to the large bandwidth of the laser pulses, the spectrum of the DFWM signal extends to the region of the CARS signal, making it difficult to detect the CARS signal. In spite of this difficulty, we have resolved a clearly separated CARS signal.

Figure 3(a) displays the energy level diagram. The employed spatial beam geometry is the folded BOXCARS configuration (see Fig. 3(b)), which allows for background-free detection of the signal. We properly choose angles between the beams such that the

phase matching condition is fulfilled. The polarizations of the pump, Stokes, and probe pulses are all set to be parallel and perpendicular to the c axis of the sapphire sample. The detection setup for the fs-CARS signal consists of a spectrometer (Bruker Optics 500 IS/SM) in which the signal is spectrally dispersed and a charge-coupled device (CCD) camera (Andor DU440-BU2) for the simultaneous detection of all spectral components. Because of the broadband laser pulses, the spectrally dispersed transient fs-CARS signal is recorded two-dimensionally, i.e., as a function of the probe pulse delay time τ and the CARS wavelength.

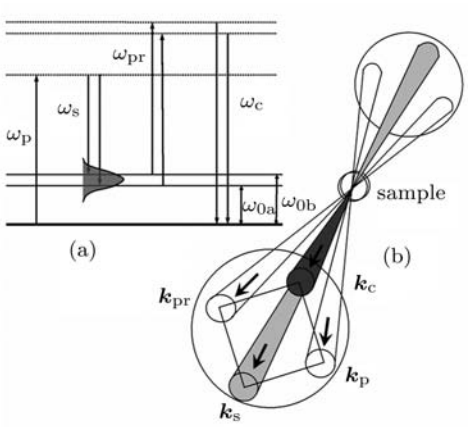


Fig. 3. Energy level diagram of the fs-CARS (a), and folded BOXCARS configuration (b).

4. Results and discussion

Firstly, we discuss the fs-CARS signal of 645-cm^{-1} and 750-cm^{-1} phonon modes in detail. Figure 4 shows the typical spectrally dispersed fs-CARS signal. The signal is plotted as a function of the probe pulse delay time τ and the CARS wavelength. After an initial fast rise and fall essentially limited by the system response function and due to the electronic nonlinear response of the crystal, the coherent phonon process appears. However, the electronic response is so strong that the coherent phonon part is difficult to observe. In order to eliminate the strong instantaneous electronic contribution in studying the coherent phonons, we further analyse the obtained data starting from the delay time of 300 fs. The contour map is shown in Fig. 5. The signal extends from about 750 nm to 770 nm and shows the expected quantum beat phenomenon. The spectrally dispersed CARS signal is centred at 758 nm, corresponding to an excitation wavenumber of 693 cm^{-1}. This is approximately the arithmetic mean wavenumber of the 645-cm^{-1} and 750-cm^{-1} modes. In order to obtain the accurate information about the phonon dynamics, the temporal evolution of fs-CARS signal at the spectral position of 758 nm is extracted (see Fig. 6.) The well-defined quantum beat signal has a period of ∼333 fs, which is in good agreement with the frequency difference of the 645-cm^{-1} and 750-cm^{-1} modes.

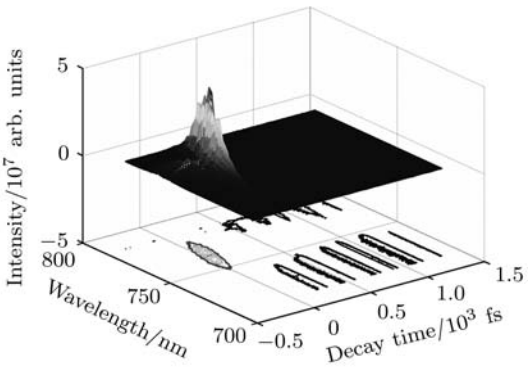


Fig. 4. Spectrally dispersed fs-CARS signal of sapphire sample.

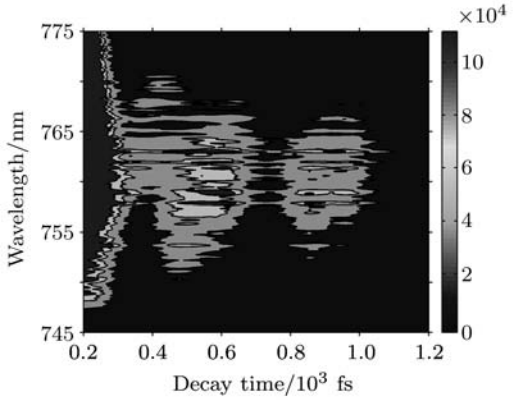


Fig. 5. Contour map of fs-CARS signal originating from the contribution of coherent phonons.

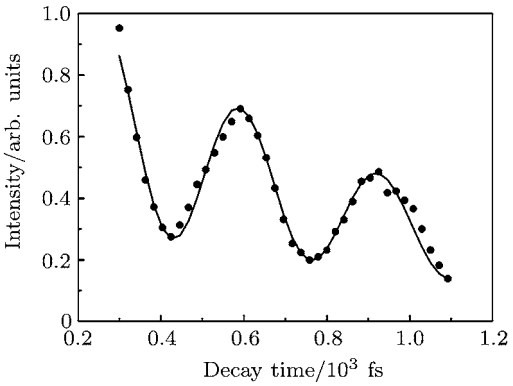


Fig. 6. Transient fs-CARS signal of 645-cm^{-1} and 750-cm^{-1} modes (solid circle) and the fitted result (solid line).

The theoretical formulas permit the numerical analysis of the experimental data. For the case of two

excited vibrational modes, $Q_{\rm tot}(t)$ in Eq. (11) can be written as

$$Q_{\rm tot}(t) = Q_{\rm a}(t) + Q_{\rm b}(t). \tag{12}$$

Using formula (7), we obtain

$$\begin{aligned} &|Q_{\rm tot}(t)|^2 \\ &\propto |Q_{0\rm a}\exp(-t/T_{2\rm a} - {\rm i}\omega_{0\rm a}t + {\rm i}\varphi_{\rm a}) \\ &\quad + Q_{0\rm b}\exp(-t/T_{2\rm b} - {\rm i}\omega_{0\rm b}t + {\rm i}\varphi_b)|^2. \end{aligned} \tag{13}$$

Equation (9) can be recast into the form

$$\begin{aligned} I_{\rm c}(\tau) \propto\ & Q_{0\rm a}^2\exp(-2\tau/T_{2\rm a}) + Q_{0\rm b}^2\exp(-2\tau/T_{2\rm b}) \\ & + 2Q_{0\rm a}Q_{0\rm b}\cos(\Delta\omega\tau + \Delta\varphi) \\ & \times \exp(-\tau(T_{2\rm a}+T_{2\rm b})/T_{2\rm a}T_{2\rm b}). \end{aligned} \tag{14}$$

When the incident excitation pulses have passed through the sapphire crystal, the stimulated excitation process rapidly terminates, the phonon modes oscillate with their respective resonance frequencies and relax freely. According to the theoretical model, we can obtain the information about the frequency difference $\Delta\omega$ of the excited modes and their respective dephasing times from the quantum beating signal. The frequency difference $\Delta\omega$ between the two excited modes we obtained from the fit procedure is 100 cm^{-1}, which coincides with the wavenumber difference of the 645-cm^{-1} and 750-cm^{-1} phonon modes. The dephasing times $T_{2\rm a}$ and $T_{2\rm b}$, for the two contributing modes, are determined to be 2600 fs and 1300 fs, respectively. According to the relationship between phonon dephasing time and phonon linewidth of the spontaneous Raman scattering,[26] as well as the ratio of amplitude $Q_{0\rm a}$ to $Q_{0\rm b}$,[12] we are able to assign the longer dephasing time $T_{2\rm a}$ to 645-cm^{-1} mode and the shorter one $T_{2\rm b}$ to 750-cm^{-1} mode. The phase relaxation process (T_2) of coherent phonons consists of pure dephasing (T_2^*) process which only destroys the vibrational coherence, and the population relaxation (T_1) process. The transient CARS signal provides the information about the overall value for the dephasing time $1/T_2 = 1/T_2^* + 1/T_1$.[26] Pure dephasing in the sapphire crystal results from scattering at boundary and lattice imperfections, and population decay is caused by anharmonic interactions.

The phase factor φ_j of excited phonon mode is related to the excitation process and determined by two factors: the pulse duration and the frequency mismatch $(\omega_{\rm p} - \omega_{\rm s}) - \omega_{0\rm j}$ between the frequency difference $\omega_{\rm p} - \omega_{\rm s}$ of the excitation pulses and the resonance frequency $\omega_{0\rm j}$ of individual phonon mode.[26] In our experiment, the ultrabroadband WLC is used for the Stokes pulse, the frequency difference $\omega_{\rm p} - \omega_{\rm s}$ can match well with both 645-cm^{-1} and 750-cm^{-1} phonons, i.e., $(\omega_{\rm p} - \omega_{\rm s}) - \omega_{0j} = 0$, the modes are resonantly excited.[18,27] For the case of good frequency match and very short femtosecond excitation pulses, the excitation pulses prepare the different coherent vibrational modes with equal initial phase, but begin to oscillate out of phase with each other after impulsive excitation due to the difference between their frequencies.[26] From the numerical fit, we obtain the phase shift $\Delta\varphi$ between the simultaneously excited 645-cm^{-1} and 750-cm^{-1} phonon modes at the delay time of the probe pulse $\tau = 0$, which is 0.6π.

For the 379-cm^{-1} and the 418-cm^{-1} phonon modes, because of the relatively low energy of the phonon modes and the broad bandwidth of femtosecond laser pulses, a spectral overlap of the pulses is generated. We obtained a very large DFWM signal making it difficult to detect the CARS signal. In spite of this difficulty, we are able to obtain the transient fs-CARS signal (shown in Fig. 7) to study the phonon dynamics. Using the foregoing theoretical model, we obtain the fit results. The frequency difference between the excited modes is 43 cm^{-1}, which accords well with the wavenumber difference between the 379-cm^{-1} mode and the 418-cm^{-1} mode. The dephasing times for the two contributing modes are determined to be 800 fs and 700 fs, respectively. According to the ratio between the amplitudes,[12] we can assign the longer dephasing time to 379-cm^{-1} mode and the shorter one to 418-cm^{-1} mode. The phase shift between the two modes at the delay time $\tau = 0$ is 0.29π.

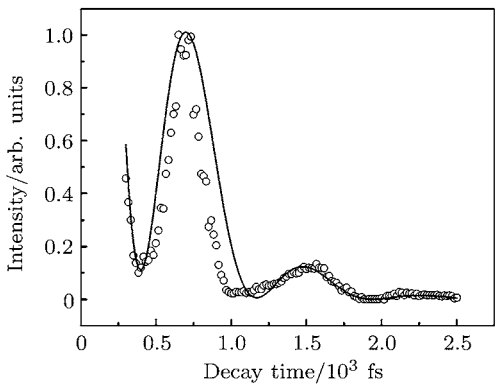


Fig. 7. Transient fs-CARS signal of 379-cm^{-1} and 418-cm^{-1} modes (open circle) and the fitted result (solid line).

5. Conclusion

In this paper, we presented fs-CARS measurement to gain the information about coherent phonon dynamics in crystals. After a theoretical description of the basic ideas of the technique, we gave experimental details, and experimental results of our sapphire sample.

Owing to the chirp structure of ultrabroadband WLC, no complicated laser system is required for the wavelength tuning of the Stokes pulse. The angles between the pump, Stokes, and probe pulses and the polarization directions of the three pulses are properly set. We have achieved the selective excitation and probing of the phonon modes. The expected quantum beat phenomenon, which is ascribed to the interference between the simultaneously excited phonon modes, is clearly observed. The theoretical formula accords well with the experimental results. The obtained dephasing times of the excited phonon modes, the wavenumber difference, and phase shift between the simultaneously excited modes are discussed. This work has proved that fs-CARS technique is a powerful tool to investigate coherent phonon dynamics in bulk crystals. It opens up the way to study directly high-frequency coherent phonon dynamics in bulk crystals on a femtosecond time scale and is of special significance to enhance our understanding of coherent phonons.

References

[1] Garrett G A, Albrecht T F, Whitaker J F and Merlin R 1996 *Phys. Rev. Lett.* **77** 3661

[2] Hase M, Mizoguchi K, Harima H, Nakashima S and Sakai K 1998 *Phys. Rev.* B **58** 5448

[3] Zeiger H J, Vidal J, Cheng T K, Ippen E P, Dresselhaus G and Dresselhaus M S 1992 *Phys. Rev.* B **45** 768

[4] Cho G C, Kütt W and Kurz H 1990 *Phys. Rev. Lett.* **65** 764

[5] Lee I H, Yee K J, Lee K G, Oh E, Kim D S and Lim Y S 2003 *J. Appl. Phys.* **93** 4939

[6] Hase M, Ishioka K, Kitajima M and Ushida K 2003 *Appl. Phys. Lett.* **82** 3668

[7] Lim Y S, Yoon S C, Yee K J, Ahn Y H, Oh E and Lee J H 2003 *Appl. Phys. Lett.* **82** 2446

[8] Chwalek J M, Uher C, Whitaker J F, Mourou G A and Agostinelli J A 1991 *Appl. Phys. Lett.* **58** 980

[9] Krauss T D and Wise F W 1997 *Phys. Rev. Lett.* **79** 5102

[10] Kano H and Hamaguchi H 2004 *Appl. Phys. Lett.* **85** 4298

[11] Wang Y H, Peng Y J, He X, Song Y F and Yang Y Q 2009 *Chin. Phys.* B **18** 1463

[12] Heid M, Schlücker S, Schmitt U, Chen T, Schweitzer-Stenner R, Engel V and Kiefer W 2001 *J. Raman Spectrosc.* **32** 771

[13] Pestov D, Zhi M C, Sariyanni Z E, Kalugin N G, Kolomenskii A, Murawski R, Rostovtsev Y V, Sautenkov V A, Sokolov A V and Scully M O 2006 *J. Raman Spectrosc.* **37** 392

[14] Meyer S, Schmitt M, Materny A, Kiefer W and Engel V 1997 *Chem. Phys. Lett.* **281** 332

[15] Meyer S and Engel V 2000 *J. Raman Spectrosc.* **31** 33

[16] Schmitt M, Knopp G, Materny A and Kiefer W 1998 *J. Phys. Chem.* A **102** 4059

[17] Rubner O, Schmitt M, Knopp G, Materny A, Kiefer W and Engel V 1998 *J. Phys. Chem.* A **102** 9734

[18] Yin J, Yu L Y, Liu X, Wan H, Lin Z Y and Niu H B 2011 *Chin. Phys.* B **20** 014206

[19] Du X, Zhang M F, Meng Q K, Song Y F, He X, Yang Y Q and Han J C 2010 *Opt. Express* **18** 22937

[20] Shen Y R 1984 *The Principles of Nonlinear Optics* (New York: Wiley)

[21] Mukamel S 1995 *Principles of Nonlinear Optical Spectroscopy* (New York: Oxford University Press)

[22] Zhang S A, Zhang H, Wang Z G and Sun Z R 2010 *Chin. Phys.* B **19** 043201

[23] Wang G G, Zhang M F, Han J C, He X D, Zuo H B and Yang X H 2008 *Cryst. Res. Technol.* **43** 531

[24] Aminzadeh A and Sarikhani-fard H 1999 *Spectrochim. Acta* A **55** 1421

[25] Kadleíková M, Breza J and Veselý M 2001 *Microelectron. J.* **32** 955

[26] Laubereau A and Kaiser W 1978 *Rev. Mod. Phys.* **50** 607

[27] Yu L Y, Yin J, Wan H, Liu X, Qu J L, Niu H B and Lin Z Y 2010 *Acta Phys. Sin.* **59** 5406 (in Chinese)